ISSN 1547-4771, Physics of Particles and Nuclei Letters, 2008, Vol. 5, No. 3, pp. 189–195. © Pleiades Publishing, Ltd., 2008.

Scaling Laws and Memory Effects in the Dynamics of Liquids and Proteins[1]

G. R. Kneller[a, b], K. Hinsen[a, b], G. Sutmann[c], and V. Calandrini[d]

[a] *Centre de Biophysique Moléculaire, CNRS,[2] Rue Charles Sadron, 45071 Orléans, France*
e-mail: kneller cnrs-orleans.fr

[b] *Synchrotron Soleil, L'Orme de Merisiers, B.P. 48, 91192 Gif-sur-Yvette, France*

[c] *Central Institute for Applied Mathematics (ZAM) and John von Neumann Institute for Computing (NIC), Research Centre Jülich, D-52425 Jülich, Germany*

[d] *Institut Laue-Langevin; 6, rue Jules Horowitz, B.P. 156; 38042 Grenoble, France*

Abstract—Recent progress in the numerical calculation of memory functions from molecular dynamics simulations allowed the gaining of deeper insight into the relaxation dynamics of liquids and proteins. The concept of memory functions goes back to the work of R. Zwanzig on the generalized Langevin equation, and it was the basis for the development of various dynamical models for liquids. In this article we present briefly a method for the numerical calculation of memory functions, which is then applied to study their scaling behavior in normal and fractional Brownian dynamics. It has been shown recently that the model of fractional Brownian dynamics constitutes effectively a link between protein dynamics on the nanosecond time scale, which is accessible to molecular dynamics simulations and thermal neutron scattering, and the much longer time scale of functional protein dynamics, which can be studied by fluorescence correlation spectroscopy.

PACS numbers: 02.60.Cb; 32.20.–r; 85.35.Lr

DOI: 10.1134/S1547477108030114

INTRODUCTION

Since the early days of computer simulations, the molecular dynamics (MD) simulation method has become a fundamental tool in the study of condensed matter systems. The 1964 paper of Anesur Rahman on a simulation study of liquid argon by MD can be considered as the pioneering work in the field [1]. Since then the method has been used in an innumerable number of studies of liquids, solids, polymer systems, molecular crystals, and biomolecules [2–4]. The history files of MD simulations contain a wealth of information, which is in many cases exploited only to a small fraction. This concerns particular simulations of biomolecular systems, where the MD method is mostly used as a sampling method in configurational space and the dynamics of the system is not considered. The purpose of this paper is to show which kind of information on the dynamical properties of complex molecular systems can be extracted from MD trajectories, and how the results can be used to develop analytical models for their dynamics. An important tool in this context is the generalized Langevin equation and the concept of memory functions, which have been introduced by Robert Zwanzig in the 1960s in order to describe the time evolution of correlation functions on a rigorous formal basis [5]. In Section 1 of this article, the concept of memory functions and their calculation from MD trajectories are briefly described. In Section 2 the method is then applied to revisit the old problem of a microscopic description of Brownian dynamics. Looking at the memory function of the velocity autocorrelation function of a tracer particle in a simple liquid, it is shown under which circumstances its dynamics can be approximated by Brownian dynamics. In Section 3 we investigate the internal dynamics of proteins and we show in particular that the latter can be described by the model of fractional Brownian dynamics. We discuss how amplitude scaling of the memory function is reflected in the self-similar behavior of the associated time correlation function. The paper is concluded by a short resumé of the results.

1. CALCULATING MEMORY FUNCTIONS FROM MD SIMULATIONS

In the following we consider a dynamical variable $U \equiv U(p, q)$, which depends on time through $2f$ phase space variables $q = \{q_1, \ldots, q_f\}$ and $p = \{p_1, \ldots, p_f\}$. Here q and p are generalized coordinates and momenta, respectively, and f is the number of degrees of freedom of the system under consideration. The autocorrelation

[1] The text was submitted by the authors in English.
[2] Affiliated with the University of Orléans.

function of U, $c_{UU}(t) = \langle U^*(0)U(t)\rangle$, can be described by an integrodifferential equation of the form [5]

$$\dot{c}_{UU}(t) = -\int_0^t d\tau M_U(t-\tau)c_{UU}(\tau), \quad (1)$$

where $M_U(.)$ is called the memory function. The latter can be related to microscopic phase space variables of the system under consideration and enables thus a rigorous formal description of relaxation processes. For practical purposes one often uses the Laplace transform of (1), which allows the relating of c_{UU} and M in Laplace space via

$$\hat{c}_{UU}(s) = \frac{c_{UU}(0)}{s + \hat{M}(s)}, \quad (2)$$

$$\hat{M}(s) = \frac{c_{UU}(0)}{\hat{c}_{UU}(s)} - s. \quad (3)$$

The Laplace transform of an arbitrary function $f(t)$ is defined as $\hat{f}(s) = \int_0^\infty dt \exp(-st)f(t)$. One recognizes immediately that the special choice $M_U(t) = \gamma_U\delta(t)$ transforms (1) into an ordinary differential equation with the solution $c_{UU}(t) = c_{UU}(0)\exp(-\gamma_U t)$. Here $\delta(t)$ is the Dirac delta distribution and $\gamma_U > 0$ is a relaxation rate. The exponential form of $c_{UU}(t)$ is characteristic for "memoryless" Markovian processes, such as Brownian dynamics.

In [6] it has been shown that autoregressive modeling of a time series $U(n\Delta t)$, which has been generated by MD, allows the extracting of the associated memory function from the analytical form of the associated time autocorrelation function. Here Δt is the sampling time step and the z-transform is the equivalent of the Laplace transform for discrete signals. For $U(n) \equiv U(n\Delta t)$, the unilateral z-transform is defined through

$$\hat{U}_>(z) = \sum_{n=0}^{\infty} U(n)z^{-n}.$$

Starting from the discretized memory function Eq. (1),

$$\frac{c_{UU}(n+1) - c_{UU}(n)}{\Delta t} = \Delta t \sum_{k=0}^{\infty} M_U(n-k)c_{UU}(k), \quad (4)$$

we obtain by z-transform the following analogue of relation (3),

$$\hat{M}_{U,>}(z) = \frac{1}{\Delta t^2}\left(z\left[\frac{c_{UU}(0)}{\hat{c}_{UU,>}(z)} - 1\right] + 1\right). \quad (5)$$

The function $\hat{c}_{UU,>}(z)$ can be obtained by using an autoregressive (AR) model for the underlying time series $U(n)$,

$$U(n) = \sum_{k=1}^{P} a_k U(n-k) + \epsilon(n). \quad (6)$$

Here $\{a_k\}$ are constant coefficients, $\epsilon(n)$ is white noise with amplitude σ, and P denotes the order of the AR model. The $P+1$ coefficients $\{a_k, \sigma\}$ can be efficiently determined by using the Burg algorithm [7, 8]. The zeros of the characteristic polynomial $p(z) = z^P - \sum_{k=1}^{P} a_k z^{P-k}$ allow to express $\hat{c}_{UU,>}(z)$ as

$$\hat{c}_{UU,>}(z) = \sum_{j=1}^{P} \beta_j \frac{z}{z - z_j}, \quad |z| > |z_j|_{\max},$$

where $|z_j|_{\max}$ is the pole with the maximum modulus and the coefficients $\{\beta_j\}$ are given by

$$\beta_j = \frac{1}{a_P} \frac{-z_j^{P-1}\sigma^2}{\prod_{k=1, k\neq j}^{P}(z_j - z_k)\prod_{l=1}^{P}(z_j - z_l^{-1})}. \quad (7)$$

From (5) the memory function can be obtained by polynomial division, using that $\hat{M}_{U,>}(z) = M(0) + M(1)z^{-1} + M(2)z^{-2} + \ldots$. We note that, within the AR model, the time correlation function $c_{UU}(n)$ has the form

$$c_{UU}(n) = \sum_{j=1}^{P} \beta_j z_j^{|n|}. \quad (8)$$

The Burg algorithm guarantees that $|z_j| < 1$, such that $\lim_{n\to\infty} c_{UU}(n) = 0$. The Fourier spectrum of $c_{UU}(t)$ can be obtained via

$$\tilde{c}_{UU}(\omega) = \Delta t \hat{c}_{UU}(\exp(i\omega\Delta t)), \quad (9)$$

where $\hat{c}_{UU}(z) = \sum_{n=-\infty}^{+\infty} c_{UU}(n)z^{-n}$ is the two-sided z-transform of $c_{UU}(n)$. The latter has the so-called "all-pole form" [8]

$$c_{UU}(z) = \frac{\Delta t\sigma^2}{\left(1 - \sum_{k=1}^{P} a_k z^{-k}\right)\left(1 - \sum_{l=1}^{P} a_l z^{l}\right)}. \quad (10)$$

2. BROWNIAN MOTION REVISITED

In the following we study the influence of the mass and the size of a tracer particle in a simple liquid on its velocity autocorrelation function (VACF) and the associated memory function [9]. The idea is in particular to gain insight into the transition from complex Hamiltonian to simple Brownian dynamics. For this purpose we consider a system of 2048 molecules of liquid argon at

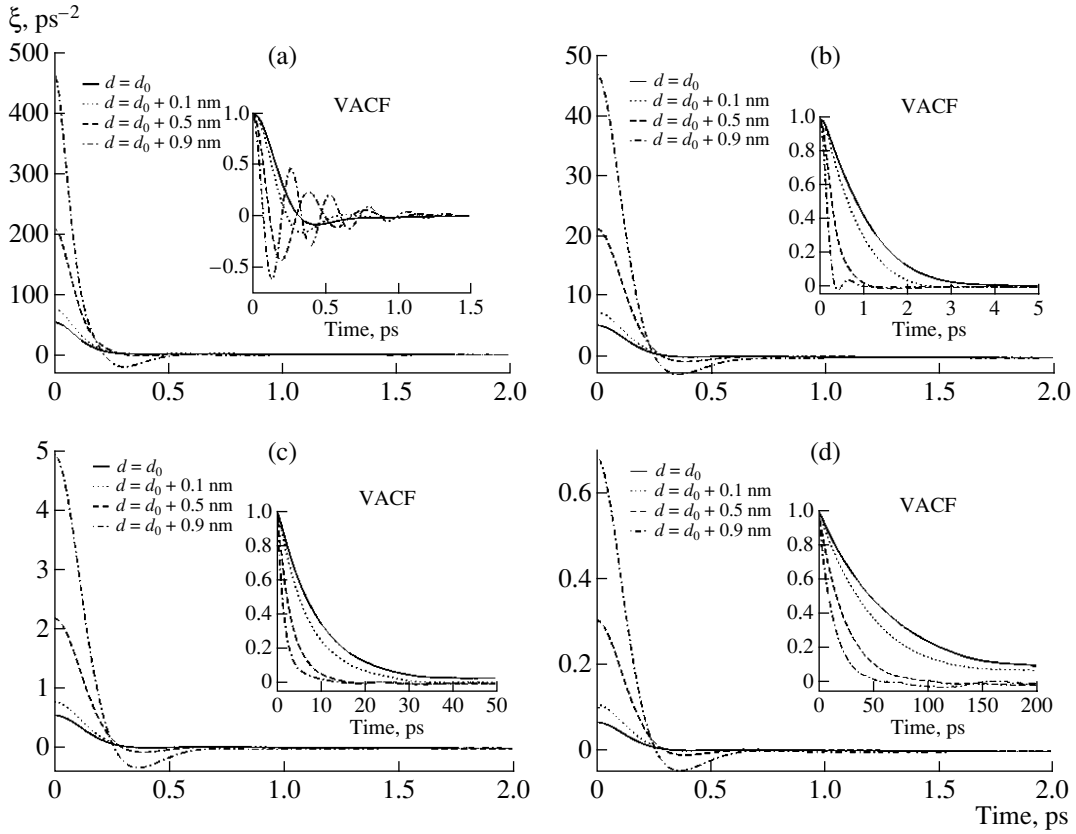

Fig. 1. Memory functions of the tracer particle for mass ratio $M/m = 1$ (a), $M/m = 10$ (b), $M/m = 100$ (c), and $M/m = 1000$ (d), respectively, and different particle sizes. The diameter of the tracer particle is $d = 2^{1/6}\sigma + \delta$ with $\sigma = 0.29599$ nm. The insets show the corresponding normalized velocity autocorrelation functions.

a temperature of 90.00 K, which interact via a simple potential of Lennard-Jones type,

$$U_{SS} = \sum_{i,\, j \in S} 4\epsilon\left(\left[\frac{\sigma}{r_{ij}}\right]^{12} - \left[\frac{\sigma}{r_{ij}}\right]^{6}\right), \tag{11}$$

$$U_{TS} = \sum_{j \in S} 4\epsilon\left(\left[\frac{\sigma}{r_{Tj} - \delta}\right]^{12} - \left[\frac{\sigma}{r_{Tj} - \delta}\right]^{6}\right). \tag{12}$$

Here "S" stands for "solvent" and "T" for "tracer particle." The parameter δ allows changing of the size of the tracer particle. The Lennard-Jones parameters are given by $\epsilon = 0.87864$ amu nm^2/ps^2 and $\sigma = 0.29599$ nm. The details of the simulation can be found in [9] and we concentrate here on the results. In the following M denotes the mass of the tracer particle and m, the one of an argon (solvent) molecule.

Figure 1 shows the memory functions of the VACF and the VACF itself (insets) for different mass ratios, ranging from $M/m = 1$ to $M/m = 1000$, and different diameters of the tracer particle, varying from $d_0 = 2^{1/6}\sigma$ to $d = d_0 + 0.9$ nm. Here d_0 defines the size of a solvent molecule. The subfigures (a)–(d) display, respectively, the results for the mass ratios $M/m = 1$, $M/m = 10$, $M/m = 100$, and $M/m = 1000$. One recognizes that increasing the particle mass reduces the amplitude of the memory function, attenuating at the same time the oscillations in the VACF, while increasing its size augments, the amplitude of the memory function, and the oscillations in the VACF. The latter reflect "rattling" motions in the cage of the next neighbors, which are more pronounced the lighter and the bigger the tracer particle is. For the minimal size d_0 and increasing mass the VACF of the tracer particle exhibits, in contrast, rapidly an exponential decay. It is important to note that the form of the associated memory function does not change with increasing mass, but just its amplitude. The latter effect can be understood for the initial value, which is given by [10]

$$M_v^{(1)}(0) = \frac{\langle F^2 \rangle}{\mu k_B T}. \tag{13}$$

Here $\langle F^2 \rangle$ is the average squared force on the tracer particle and μ its reduced mass with respect to the simulated solvent. For $M/m = 1000$ (Fig. 1d), it becomes visible that the memory function scales with the inverse reduced mass and not with the inverse mass of the tracer particle. The interesting point here is that, not only the initial value of the memory function scales with the inverse (reduced) mass, but the memory func-

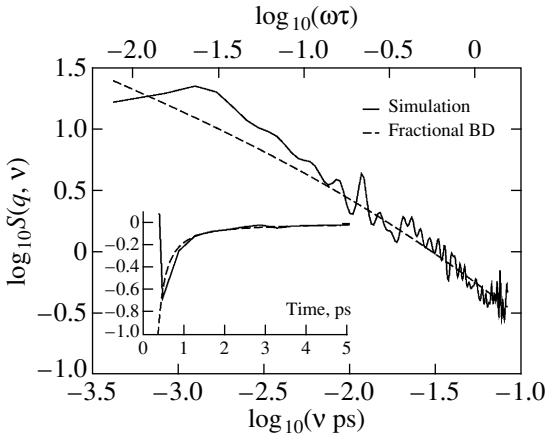

Fig. 2. Log-log plot of the coherent dynamic structure factor of lysozyme as a function of frequency for $q = 10\ \text{nm}^{-1}$. The solid line represents the simulation results and the dashed line the fitted fBD model. The parameters of the fit are $\tau = 4.0$ ps and $\beta = 0.5$.

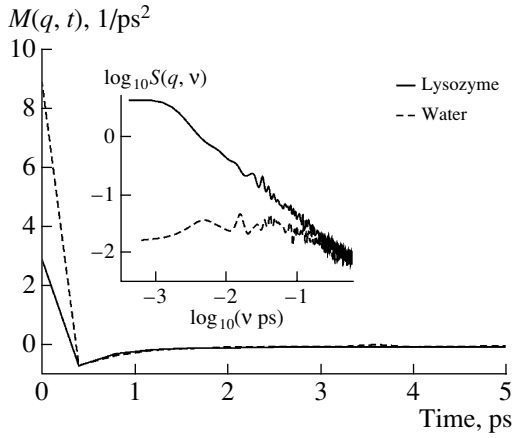

Fig. 3. Memory function of the coherent dynamic structure factor at $q = 10\ \text{nm}^{-1}$ for lysozyme (solid line) as compared to water (broken line). The inset shows the corresponding dynamic structure factors. More explanations are given in the text.

tion over the whole time scale. The observation that reducing the amplitude of the memory function leads to Brownian motion has been formalized in [11], considering a multiplication of the memory function of an arbitrary time correlation function by a scaling factor $\lambda > 0$. It follows from the linearity of the Laplace transform that $\hat{M}(s) \longrightarrow \lambda\hat{M}(s)$ (the index U is omitted), and introducing the normalized autocorrelation function

$$\psi(t) = \frac{\langle v(t)v(0)\rangle}{\langle v^2\rangle}, \tag{14}$$

the inverse Laplace transform of (2) may thus be expressed as

$$\begin{aligned}\psi_\lambda(t) &= \frac{1}{2\pi i}\oint_C ds\frac{\exp(st)}{s+\lambda\hat{M}(s)},\\ &\overset{s\to s/\lambda}{=} \frac{1}{2\pi i}\oint_{C'} ds\frac{\exp(s\lambda t)}{s+\hat{M}(\lambda s)}.\end{aligned} \tag{15}$$

The contours C and C' include the singularities of $\hat{\psi}(s)$ and $\hat{\psi}_\lambda(s)$, respectively. One sees that $\psi_\lambda(t)$ is obtained in two steps:

(1) The memory function is modified according to

$$M(t) \longrightarrow M_\lambda(t) = \frac{1}{\lambda}M\left(\frac{t}{\lambda}\right), \tag{16}$$

where one uses the scaling property of the Laplace transform, $(1/\lambda)f(t/\lambda) \longleftrightarrow \hat{f}(\lambda s)$.

(2) The modified memory function is used to evaluate the corresponding correlation function on the time scale $t \longrightarrow \lambda t$, which is "stretched" if $0 < \lambda < 1$.

For $\lambda \ll 1$ the memory function $M_\lambda(t)$ will tend to a Dirac delta distribution,

$$M_\lambda(t) \overset{\lambda\ll 1}{\longrightarrow} \gamma\delta(t), \tag{17}$$

where $\gamma = \int_0^\infty dtM_\lambda(t)$ is the friction constant. It should be noted that the transformation (16) does not change the value of the integral over the memory function. On account of relation (17), the correlation function will tend to an exponential function on the time scale λt,

$$\psi(t) \overset{\lambda\ll 1}{\longrightarrow} \exp(-\lambda\gamma t). \tag{18}$$

It must be emphasized that the limit $\lambda \longrightarrow 0$ cannot be performed formally, since the VACF would not decay at all in this limit. Since the VACF is a classical autocorrelation function, it is even in time and consequently $\dot{\psi}(0) = 0$. The exponential behavior can thus not be true for $t \longrightarrow 0$, since $\exp(-\lambda\gamma|t|)$ is not differentiable at $t = 0$. As demonstrated in [11], the limiting case of exponential decay of correlation functions must be considered on a coarse-grained time scale

$$\Delta t = 2\int_0^\infty dt\frac{M(t)}{M(0)}, \tag{19}$$

and the Brownian regime is attained if

$$\Delta t \ll \frac{1}{\sqrt{M(0)}}. \tag{20}$$

Equations (19) and (20) define the regime of Brownian Dynamics on the basis of microscopic Hamiltonian dynamics. Note that the scaling of the memory function with $\lambda < 1$—such as it occurs with increasing mass of a tracer particle—will not change the Brownian time step Δt. It will, however, change the right-hand side of con-

dition (20), such that it will be the better fulfilled the smaller λ is.

3. FRACTIONAL BROWNIAN MOTION IN PROTEINS AND WATER

Recent experimental and simulation studies have shown that fractional Brownian dynamics (fBD) is a good model to describe empirically the relaxation dynamics of proteins over an extremely wide spectrum of time scales, ranging from picoseconds to seconds [12–17]. Here the internal dynamics of proteins is considered, neglecting global translations and rotations. The corresponding time correlation functions are characterized by a strongly nonexponential decay and can be formally derived from so-called fractional Fokker-Planck equations [18]. Taking the fractional Ornstein-Uhlenbeck process as a dynamical model for the variable $U(t)$, one obtains for the normalized position autocorrelation function $\psi(t) := \langle x(t)x(0)\rangle/\langle x^2\rangle$,

$$\psi(t) = E_\beta(-[t/\tau]^\beta), \quad 0 < \beta \le 1, \tag{21}$$

where $E_\beta(z)$ is the Mittag-Leffler function of order β [19] and τ defines a time scale. The series representation of $E_\beta(z)$ has the form

$$E_\beta(z) = \sum_{n=0}^{\infty} \frac{z^n}{\Gamma(1+\beta n)}, \tag{22}$$

with $\Gamma(z)$ being the generalized factorial [19, 20]. One recognizes that $E_1(z) = \exp(z)$. The fractional Ornstein-Uhlenbeck process describes anomalously slow diffusion of a particle in a harmonic potential. The harmonic potential ensures that the motion is bound in space, which is necessary to describe atomic motions in proteins whose center of mass is fixed, and the "anomaly" is reflected in the nonexponential form of the autocorrelation function (21).

Various important properties of the time correlation function can be derived from its Laplace transform

$$\hat{\psi}(s) = \frac{1}{s(1+[s\tau]^{-\beta})}. \tag{23}$$

The Fourier spectrum of $\psi(t)$, for example, can be expressed as $\tilde{\psi}(\omega) = 2\Re\{\hat{\psi}(i\omega)\}$, and one obtains [16].

$$\tilde{\psi}(\omega) = \frac{2\tau\sin(\beta\pi/2)}{|\omega\tau|(|\omega\tau|^\beta + 2\cos(\beta\pi/2) + |\omega\tau|^{-\beta})}, \tag{24}$$

where $0 < \beta \le 1$. The Laplace transform of the associated memory function can be directly read off from (23),

$$\hat{M}(s) = s(s\tau)^{-\beta}, \tag{25}$$

and a carefully performed inverse Laplace transform yields [16]

$$M(t) = \frac{\beta-1}{\Gamma(\beta)\tau^2}\left(\frac{t}{\tau}\right)^{\beta-2}, \quad t > 0. \tag{26}$$

Although $M(t)$ becomes singular for $t \longrightarrow 0+$, the friction constant is zero

$$\gamma = \int_0^\infty dt M(t) = 0. \tag{27}$$

The above mathematical properties indicate that the memory function for fBD is a distribution and not a normal function. Figure 2 shows the Fourier transform of the coherent scattering function of lysozyme, which has been obtained from MD simulation (solid line), as compared to a fit of the fBD model (broken line). The details are described in [16]. The coherent scattering function is defined by $F(q,t) \equiv c_{UU}(q,t)$, where $U(q,t) = \sum_{j=1}^{N} \exp(iqx_j(t))$ and x_j is the x-coordinate of atom j, assuming that the scattering system is isotropic. The Fourier transform of $F(q, t)$ is referred to as the dynamic structure factor. The inset of Fig. 2 shows the associated memory function and the corresponding fit of expression (26). The analysis has been performed by using an AR model with 400 poles and a sampling step of $\Delta t = 0.4$ ps. One recognizes well that the overall form of the simulated dynamic structure factor has the featureless form of the model spectrum, and that the characteristic algebraic form of the memory function is retrieved in the simulation results.

The fractal behavior of fBD on the time scale can be understood by using the scaling properties of the corresponding memory function [21]. It follows from Eq. (25) that

$$\hat{M}(\lambda s) = \lambda^{1-\beta}\hat{M}(s), \tag{28}$$

and using this relation in conjunction with Eq. (15) allows us to write

$$\psi_\lambda(t) = \frac{1}{2\pi i}\oint_C ds \frac{\exp(st)}{s+\lambda\hat{M}(s)},$$

$$\overset{s\to s/\lambda}{=} \frac{1}{2\pi i}\oint_{C'} ds \frac{\exp(s\lambda t)}{s+\lambda^{1-\beta}\hat{M}(s)}.$$

Now one can again apply the same argument, which has been used to derive the second line of (15) from the first

one, and iterating this procedure for n steps yields

$$\psi_\lambda(t) = \frac{1}{2\pi i}\oint_C ds \frac{\exp(st)}{s + \lambda\hat{M}(s)} = \frac{1}{2\pi i}\oint_{C'} ds \frac{\exp\left(st\lambda^{\sum_{j=0}^{n-1}(1-\beta)^j}\right)}{s + \hat{M}(s\lambda^{(1-\beta)^{n-1}})}.$$

For $0 < \beta < 1$, it follows that $\lim_{n\to\infty}\lambda^{(1-\beta)^{n-1}} = 1$ and the geometrical series $\sum_{j=0}^{\infty}(1-\beta)^j$ converges to $1/(1-[1-\beta]) = 1/\beta$. Therefore we obtain finally

$$\psi_\lambda(t) = \psi(\lambda^{1/\beta}t). \quad (29)$$

In contrast to normal Brownian dynamics, amplitude scaling of the memory function yields the same time correlation function just on a different time scale. This explains why spectroscopic techniques operating on very different time scales can reveal the same relaxation behavior. Apart from an amplitude factor, they all see the same memory function. In this context we mention fluorescence correlation spectroscopy and quasielastic neutron scattering, which are sensitive to relaxation processes on the submillisecond to the second range [13–15] and to the pico- to nanosecond range, respectively [17].

Fractional Brownian dynamics is not a special property of proteins, but can also be found as a component in the dynamics of ordinary liquids. As an example we consider the memory function of the coherent scattering function of liquid (bulk) water, which has been obtained by using the same parameters as in the analyses of the MD simulations of lysozyme discussed above. The simulations of water have been performed for 256 water molecules in a cubic box of edge length 1.9552 nm in the thermodynamic *NpT*-ensemble at a temperature of $T = 300$ K and a pressure of 1 bar, using the SPC/E potential [22] and Ewald summation for long-range electrostatic interactions. Within the SPC/E model, the water molecules are treated as rigid bodies which are composed of point masses, carrying each an electric charge. All simulations have been performed with the simulation program DL_POLY (version 2) [23], using a simulation time step of 1 fs. Figure 3 shows that the memory functions for lysozyme and water are almost identical for $t \geq \Delta t$. Here $\Delta t = 0.4$ ps is the sampling time step we used in both cases for the AR analysis and which sets the resolution of the AR model. Within the numerical resolution, the only difference between the memory functions for water and lysozyme is the behavior at short times, which yields different friction constants. We find

$$\gamma_{H_2O} = 2.05\ \text{ps}^{-1}, \quad (30)$$

$$\gamma_{Lys} = 0.07\ \text{ps}^{-1}. \quad (31)$$

The latter value being close to zero is another indication for "pure" fBD in lysozyme, whereas $\gamma_{H_2O} > 0$ indicates that there is an additional relaxation channel in water, which may be attributed to the diffusion of water molecules.

CONCLUSIONS

In this article we have demonstrated that the calculation of memory functions from MD simulations of molecular systems allows discrimination between different dynamical models in a more rigorous way than standard analyses of the associated time correlation functions and their Fourier spectra. One obtains in particular a systematic description of relaxation processes in complex systems. Using autoregressive analysis of MD trajectories, we have first revisited the old problem of Brownian dynamics. We have demonstrated that the memory function of a tracer particle scales inverse proportionally with its mass and that it is this effect that leads to the characteristic exponentially decaying velocity autocorrelation function of Brownian dynamics when the mass is increased. The scaling behavior of the memory function for normal Brownian dynamics has been opposed to the one for fractional Brownian dynamics. We have in particular shown that in case fBD scaling of the memory function does not lead to a change of the form of the associated time correlation function, but just to a change of the time scale for the latter. This reflects the fractal character of fBD and explains why spectroscopic techniques operating on very different time scales see the same relaxation behavior. Using preliminary results from analyses of MD simulations of liquid water, we have demonstrated that fBD is also present in normal liquids, with an additional relaxation channel due to unbound diffusion of the molecules. These preliminary results suggest in particular that the relaxation dynamics of proteins is strongly coupled to the one of the surrounding solvent, and more detailed analyses will be published in a forthcoming paper.

REFERENCES

1. A. Rahman, Phys. Rev. **136** (2A), 405–411 (1964).
2. G. Ciccotti, D. Frenkel, and I. R. McDonald, *Simulation of Liquids and Solids* (North-Holland, Amsterdam, 1987).
3. M. P. Allen and D. J. Tildesley, *Computer Simulation of Liquids* (Oxford Univ., Oxford, 1987).
4. D. Frenkel and B. Smith, *Understanding Molecular Simulation* (Academic, London, San Diego, 1996).
5. R. Zwanzig, *Statistical Mechanics of Irreversibility*, Lectures in Theor. Phys. (Wiley, New York, 1961), pp. 106–141.
6. G. R. Kneller and K. Hinsen, J. Chem. Phys. **115** (24), 11097–11105 (2001).

7. J. Burg, "Maximum Entropy Spectral Analysis," PhD Thesis (Stanford Univ., Stanford, CA, USA, 1975).
8. A. Papoulis, *Probablity, Random Variables, and Stochastic Processes*, 3rd ed. (McGraw Hill, 1991).
9. G. R. Kneller, K. Hinsen, and G. Sutmann, J. Chem. Phys. **118** (12), 5283–5286 (2003).
10. P. Espanol and I. Zuniga, J. Chem. Phys. **98** (1), 574–580 (1992).
11. G. R. Kneller and G. Sutmann, J. Chem. Phys. **120** (4), 1667–1669 (2004).
12. W. G. Glöckle and T.F. Nonnenmacher, Biophys. J. **68**, 46–53 (1995).
13. H. Yang and X. S. Xie, J. Chem. Phys. **117** (24), 10965–10979 (2002).
14. H. Yang, G. Luo, P. Karnchanaphanurach, et al., Science **302** (5643), 262–266 (2003).
15. S. C. Kou and X. S. Xie, Phys. Rev. Lett. **93**, 180603 (2004).
16. G. R. Kneller and K. Hinsen, J. Chem. Phys. **121** (20), 10278–10283 (2004).
17. G. R. Kneller, Phys. Chem. **7**, 2641–2655 (2005).
18. R. Metzler and J. Klafter, Phys. Rev. E **61** (6), 6308–6311 (2000).
19. A. Erdelyi, W. Magnus, F. Oberhettinger, and F. G. Tricomi, *Higher Transcendental Functions* (McGraw Hill, 1955).
20. M. Abramowitz and I. A. Stegun, *Handbook of Mathematical Functions* (Dover Publications, New York, 1972).
21. G. R. Kneller and V. Calandrini, Manuscript submitted.
22. H. J. C. Berendsen, J. R. Grigera, and T. P. Straatsma, J. Phys. Chem. **9**, 6269–6270 (1987).
23. W. Smith, C. W. Yong, and P. M. Rodger, Molecular Simulation **28** (1), 385–471 (2002).